Mapping the Position of DNA Polymerase-Bound DNA Templates in a Nanopore at 5 Å Resolution

Brett Gyarfas,[†] Felix Olasagasti,[‡] Seico Benner,[‡] Daniel Garalde,[†] Kate R. Lieberman,[‡] and Mark Akeson[‡,*]

[†]Department of Computer Engineering and [‡]Department of Biomolecular Engineering, Baskin School of Engineering, University of California, Santa Cruz, California 95064

ARTICLE

ABSTRACT DNA polymerases are molecular motors that catalyze template-dependent DNA replication, advancing along template DNA by one nucleotide with each catalytic cycle. Nanopore-based measurements have emerged as a single molecule technique for the study of these enzymes. Using the α-hemolysin nanopore, we determined the position of DNA templates bearing inserts of abasic (1′,2′-dideoxy) residues, bound to the Klenow fragment of *Escherichia coli* DNA polymerase I (KF) or to bacteriophage T7 DNA polymerase. Hundreds of individual polymerase complexes were analyzed at 5 Å precision within minutes. We generated a map of current amplitudes for DNA—KF—deoxynucleoside triphosphate (dNTP) ternary complexes, using a series of templates bearing blocks of three abasic residues that were displaced by ~5 Å in the nanopore lumen. Plotted as a function of the distance of the abasic insert from $n = 0$ in the active site of the enzyme held atop the pore, this map has a single peak. The map is similar when the primer length, the DNA sequences flanking the abasic insert, and the DNA sequences in the vicinity of the KF active site are varied. Primer extension catalyzed by KF using a three abasic template in the presence of a mixture of dNTPs and 2′,3′-dideoxynucleoside triphosphates resulted in a ladder of ternary complexes with discrete amplitudes that closely corresponded to this map. An ionic current map measured in the presence of 0.15 M KCl mirrored the map obtained with 0.3 M KCl, permitting experiments with a broader range of mesophilic DNA and RNA processing enzymes. We used the abasic templates to show that capture of complexes with the KF homologue, T7 DNA polymerase, yields an amplitude map nearly indistinguishable from the KF map.

KEYWORDS: Klenow fragment · T7 DNA polymerase · nanopore · α-hemolysin · single molecule · DNA-binding proteins

DNA polymerases catalyze template-dependent DNA replication. These enzymes are molecular motors that advance by one nucleotide along template DNA with each catalytic cycle. Kinetic studies of the Klenow fragment of *Escherichia coli* DNA polymerase I (KF), an A-family polymerase, have shown that in an ordered assembly mechanism KF recognizes the double strand−single strand junction of its DNA substrate to form a binary complex, to which deoxynucleoside triphosphate (dNTP) then binds to form a ternary complex.[1] Crystal structures of A-family polymerases have revealed a conserved catalytic domain that resembles a partially open right hand.[2] The palm subdomain contains residues essential for catalysis, the thumb subdomain positions the primer/template DNA duplex in the active site, and the fingers subdomain is essential for binding dNTP substrates. Structures of binary and ternary complexes show that a conformational transition occurs between these two functional states.[3−5] In ternary complexes, the fingers subdomain rotates in toward the active site, forming a tight steric fit with the nascent base pair. In the ternary complex, the affinity of KF for its DNA substrate is increased by ~5- to 8-fold.[6]

Nanopore-based measurements have emerged as a single molecule technique for the study of DNA polymerases.[7−9] Nanoscale pores may be etched in solid-state substrates such as silicon nitride,[10] but the highest precision measurements are made using protein pores inserted in lipid bilayers.[7,11−14,15] Figure 1a illustrates a single pore formed by an α-hemolysin (α-HL) heptamer. The limiting aperture of the pore is just sufficient to accommodate single-stranded DNA, while the adjacent pore vestibule can accommodate double-stranded (duplex) DNA.[16,17] Absent DNA, the open channel ionic current (I_o) through the α-HL pore is 60 pA at 180 mV applied potential in 0.3 M KCl. Voltage-dependent capture of a complex of DNA with KF results in a decreased current corresponding to the enzyme-bound state (EBS). In this state (I_{EBS}, Figure 1b,i), KF holds the duplex portion of the DNA substrate atop the pore, with the single-stranded template suspended in the transmembrane pore lumen.[8] Upon voltage-promoted KF dissociation, the duplex DNA drops down into the pore vestibule, causing a further decrease in current (I_{DNA}, Figure 1b,ii). The event is terminated by electrophoresis of the DNA

*Address correspondence to makeson@soe.ucsc.edu.

Received for review March 26, 2009 and accepted May 21, 2009.

Published online June 2, 2009.
10.1021/nn900303g CCC: $40.75

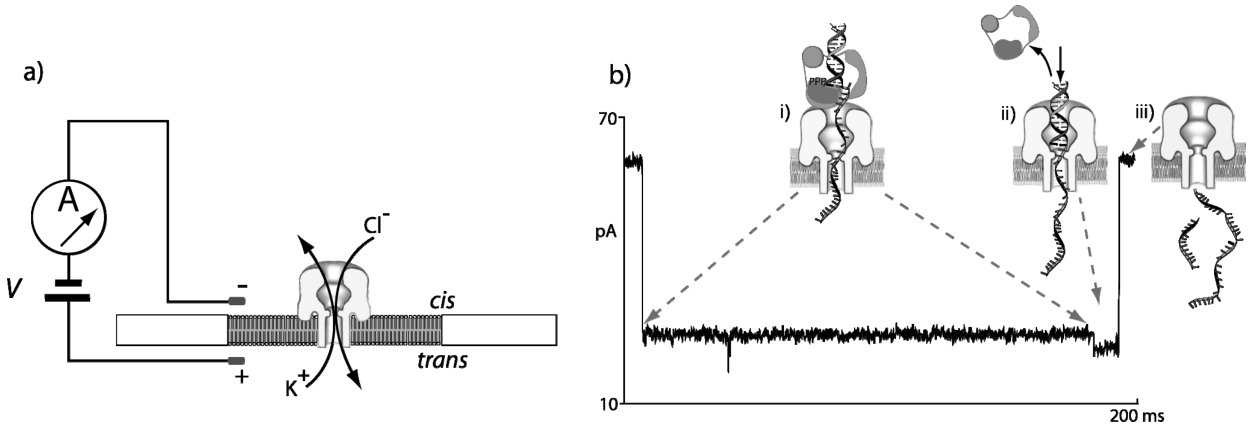

Figure 1. Detection of nanopore capture events. (a) Illustration of the nanopore device. A patch-clamp amplifier supplies voltage and measures ionic current through a single α-HL channel inserted in a ~25 μm diameter lipid bilayer (*trans*-side positive). Current through the nanopore is carried by K^+ and Cl^- ions. (b) Representative current trace at 180 mV for nanopore capture of a KF−DNA complex. Cartoons in b illustrate the molecular events corresponding to each current level: (i) Initial long blockade is the enzyme-bound state (EBS), during which the duplex DNA is held atop the pore vestibule due to association with KF. (ii) Shorter 20 pA terminal step occurs when KF dissociates and the duplex DNA drops into the nanopore vestibule. (iii) DNA strands translocate through the nanopore, resulting in a return to the open channel current.

through the pore, restoring the open channel current (Figure 1b,iii). Dwell time and average amplitude in each current state are typically reported in nanopore experiments.[18,19]

We have shown that DNA−KF complexes held atop the α-HL nanopore in an electric field iteratively bind and release dNTP substrate, leading to a dNTP concentration-dependent increase in EBS dwell time.[9] This binding is dependent upon complementarity to the template base in the polymerase active site and is a requirement for monitoring DNA synthesis in real time using nanopore technology. The ability to discern nucleotide incorporation is also required to observe synthesis in this configuration. One strategy to achieve this is to detect template displacement, ideally with single nucleotide (5 Å) precision. In this scenario, the enzyme complex is held atop the pore under applied voltage, and the DNA substrate is drawn up through the nanopore by the distance of a single nucleotide with each catalytic cycle.

In this study, we describe the use of DNA templates bearing inserts of abasic (1′, 2′-dideoxy) residues (Figure 2) to monitor the position of DNA substrates bound to KF and T7 DNA polymerase, captured in the α-HL nanopore. Hundreds to thousands of individual polymerase complexes were analyzed at 5 Å precision within minutes under ambient conditions. With this technique, we determined a map of current amplitudes for KF ternary complexes using templates bearing blocks of three abasic residues that are displaced by ~5 Å in the nanopore lumen. This map has a single peak. The map is similar when the primer length, the

A. DNA	**5'-CTCACCTATCCTTCCACTCATTCCAATTAATTACCATTCATTCAGATCTCACTATCGCATTCTCATGCAGGTCGTAGCC-3'**
B. 12ab(12,23)	**5'-**CTCACCTATCCTTCCACTCATTCCAATTAATT**XXXXXXXXXXXX**GATCTCACTATCGCATTCTCATGCAGGTCGTAGCC**-3'**
C. 6ab(18,23)	**5'-**CTCACCTATCCTTCCACTCATTCCAATTAATT**XXXXXX**CATTCAGATCTCACTATCGCATTCTCATGCAGGTCGTAGCC**-3'**
D. 6ab(12,17)	**5'-**CTCACCTATCCTTCCACTCATTCCAATTAATTACCATT**XXXXXX**GATCTCACTATCGCATTCTCATGCAGGTCGTAGCC**-3'**
E. 3ab(6,8)	**5'-**CTCACCTATCCTTCCACTCATTCCAATTAATTACCATTCATTCAGAT**XXX**ACTATCGCATTCTCATGCAGGTCGTAGCC**-3'**
F. 3ab(7,9)	**5'-**CTCACCTATCCTTCCACTCATTCCAATTAATTACCATTCATTCAGA**XXX**CACTATCGCATTCTCATGCAGGTCGTAGCC**-3'**
G. 3ab(8,10)	**5'-**CTCACCTATCCTTCCACTCATTCCAATTAATTACCATTCATTCAG**XXX**TCACTATCGCATTCTCATGCAGGTCGTAGCC**-3'**
H. 3ab(9,11)	**5'-**CTCACCTATCCTTCCACTCATTCCAATTAATTACCATTCATTCA**XXX**CTCACTATCGCATTCTCATGCAGGTCGTAGCC**-3'**
I. 3ab(10,12)	**5'-**CTCACCTATCCTTCCACTCATTCCAATTAATTACCATTCATTC**XXX**TCTCACTATCGCATTCTCATGCAGGTCGTAGCC**-3'**
J. 3ab(11,13)	**5'-**CTCACCTATCCTTCCACTCATTCCAATTAATTACCATTCATT**XXX**ATCTCACTATCGCATTCTCATGCAGGTCGTAGCC**-3'**
K. 3ab(12,14)	**5'-**CTCACCTATCCTTCCACTCATTCCAATTAATTACCATTCAT**XXX**GATCTCACTATCGCATTCTCATGCAGGTCGTAGCC**-3'**
L. 3ab(13,15)	**5'-**CTCACCTATCCTTCCACTCATTCCAATTAATTACCATTCA**XXX**AGATCTCACTATCGCATTCTCATGCAGGTCGTAGCC**-3'**
M. 3ab(14,16)	**5'-**CTCACCTATCCTTCCACTCATTCCAATTAATTACCATTC**XXX**CAGATCTCACTATCGCATTCTCATGCAGGTCGTAGCC**-3'**
N. 3ab(15,17)	**5'-**CTCACCTATCCTTCCACTCATTCCAATTAATTACCATT**XXX**TCAGATCTCACTATCGCATTCTCATGCAGGTCGTAGCC**-3'**
O. 3ab(16,18)	**5'-**CTCACCTATCCTTCCACTCATTCCAATTAATTACCAT**XXX**TTCAGATCTCACTATCGCATTCTCATGCAGGTCGTAGCC**-3'**
P. 3ab(17,19)	**5'-**CTCACCTATCCTTCCACTCATTCCAATTAATTACCA**XXX**ATTCAGATCTCACTATCGCATTCTCATGCAGGTCGTAGCC**-3'**
Q. 3ab(18,20)	**5'-**CTCACCTATCCTTCCACTCATTCCAATTAATTACC**XXX**CATTCAGATCTCACTATCGCATTCTCATGCAGGTCGTAGCC**-3**

Figure 2. DNA template oligonucleotides used in this study. In each sequence, X indicates the positions of the abasic (1′,2′-dideoxy) residues. Abasic configuration is denoted as *N*ab(*x*,*y*), where *N* is the number of abasic residues in the insert, and *x* and *y* indicate the distance (in nucleotides) of the first and last abasic residues of the insert, measured from the dNMP at *n* = 0 in the polymerase catalytic site. Note that this configuration changes when the same template is hybridized to primers of different lengths. For example, the abasic identity for template J is 3ab(11,13) with a 23mer primer, 3ab(12,14) with a 22mer primer, and 3ab(10,12) with a 24mer primer. The 23mer primer binding sequence is shown underlined in the all DNA template. The abasic configuration for each template when it is annealed with a 23mer primer is indicated to the left of each sequence.

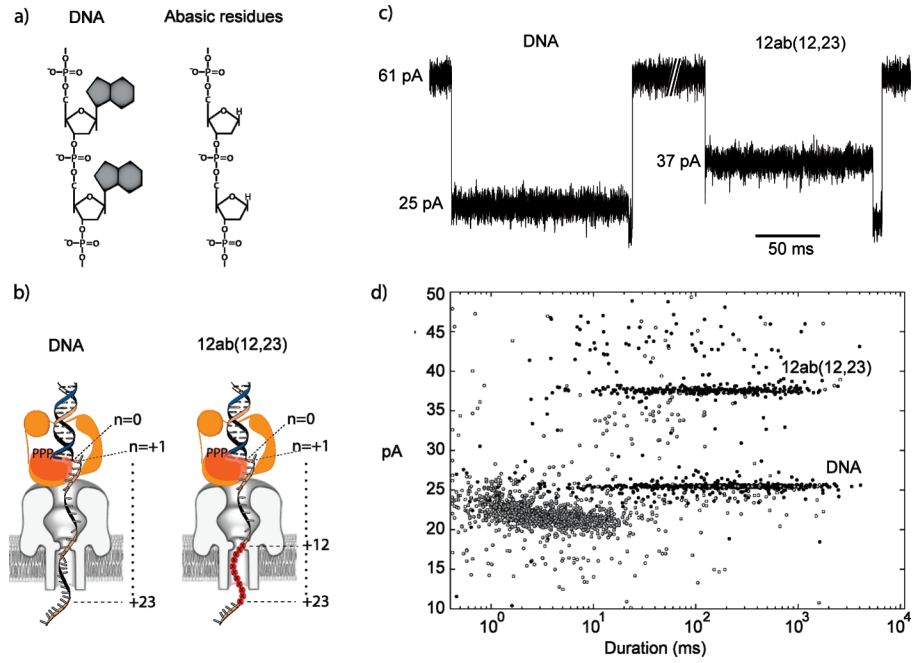

Figure 3. Detection of abasic residues in DNA templates bound to KF and captured in the nanopore. (a) Comparison of abasic and standard DNA residues. A section of standard DNA strand, with nucleobases at the 1′ position represented as unsubstituted purines, and a section of a strand bearing abasic (1′,2′-dideoxy) residues. (b) Illustration of DNA−KF−dNTP ternary complexes captured on the nanopore, formed with templates containing either all DNA or a 12 abasic residue insert (12ab(12,23)), hybridized to a 23mer 2′,3′-dideoxy-terminated primer. Each abasic monomer is drawn as a red circle with a black X inside. The distance from the first template base ($n = 0$) in the KF active site along the template strand that extends through the nanopore lumen is indicated. (c) Characteristic current traces of capture events for the two complexes shown in b. (d) Dwell time *vs* amplitude plot for capture events of the two complexes shown in b. Black dots indicate the EBS of events, gray dots, the terminal current steps of events, and white dots with black outline are events without terminal current steps.

DNA sequences flanking the abasic insert, and the DNA sequences in the vicinity of the KF active site are varied. The ionic current map measured in the presence of 0.15 M KCl mirrored the map obtained with 0.3 M KCl, permitting experiments with a broader range of mesophilic enzymes. Using these abasic-containing templates, we found that capture of complexes with the KF homologue, T7 DNA polymerase, yields a map that is nearly indistinguishable from the KF map. Finally, primer extension catalyzed by KF using an abasic-containing template in the presence of a mixture of dNTPs and 2′,3′-dideoxynucleoside triphosphates (ddNTPs) resulted in a ladder of ternary complexes with discrete amplitudes that closely corresponded to this map. Thus enzymatic products generated using the biochemical strategy for DNA sequencing pioneered by Sanger[20] were displayed using the nanopore.

RESULTS

Detection of Abasic Segments within DNA. Our initial objective was to design a primer/template substrate that when bound to KF and captured atop the α-HL pore resulted in a current signature distinguishable from standard DNA. We reasoned that a segment of abasic residues near the limiting aperture of the α-HL channel would impede ionic current through the pore less than DNA residues. This is because the volume occupied by each abasic monomer is significantly less than DNA nucleotides while retaining the same spacing and charge density. We used the dimensions of the nanopore,[16] the length of single-stranded DNA, and the location of the double strand−single strand DNA junction when a captured substrate molecule is bound to KF[8] (Figure 1b) to design a template with a block of 12 abasic (2′-dideoxy) residues (Figure 2, template B). We predicted that when hybridized to a 23mer primer, bound to KF, and captured atop the nanopore, the abasic segment of this template would reside in the nanopore lumen (Figure 3b). Throughout this study, the abasic configuration of substrates is denoted as *N*ab(*x*,*y*), where *N* is the number of abasic residues in the insert, and *x* and *y* indicate the distance (in nucleotides) from the dNMP at $n = 0$ in the polymerase catalytic site to the first and last abasic residues of the insert, respectively (Figure 2). Thus for this substrate, the designation 12ab(12,23) indicates that the abasic segment spans residues +12 to +23 relative to template position $n = 0$ in the polymerase active site.

We compared nanopore events for DNA−KF−dNTP ternary complexes formed with the 12ab(12,23) substrate to those obtained with the corresponding all DNA substrate (Figure 2, template A). Both templates were hybridized to a 23mer 2′,3′-dideoxy-terminated primer. The dideoxy terminus prevents phosphodiester bond formation while permitting tight dNTP binding. Thus in the presence of 200 μM dGTP (the complement

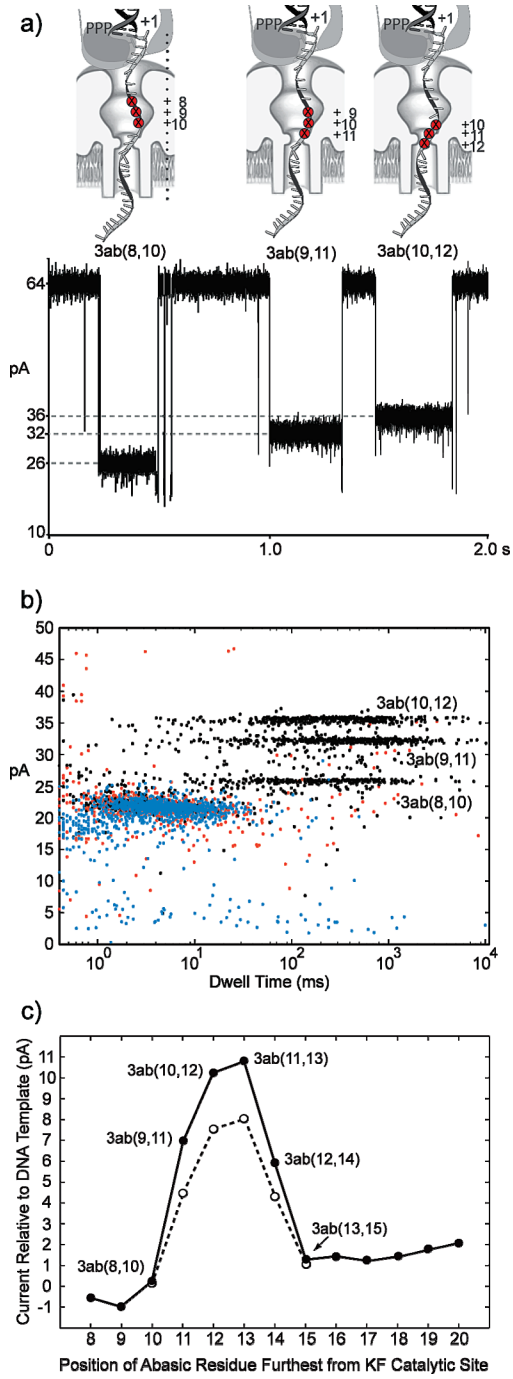

Figure 4. Mapping a three abasic residue template segment in the nanopore lumen. (a) Illustration (above) and corresponding current traces (below) for the capture of DNA−KF−dGTP ternary complexes formed with templates bearing three abasic residue inserts. Templates were hybridized to a 23mer primer, yielding the indicated abasic configurations. Abasic monomers are illustrated with a black X inside a red circle. (b) Dwell time *vs* amplitude plot for the experiment yielding the current traces shown in a. Black dots indicate the EBS of events, blue dots are the terminal current steps of events, and red dots are events without terminal current steps. (c) Map of current levels for KF ternary complexes formed with a series of templates (Figure 2, templates E−Q) in which a three abasic residue insert was displaced in single nucleotide increments. Maps measured in buffer containing 0.3 M KCl (solid line) or 0.15 M KCl (dashed line) are shown. EBS amplitudes were normalized to the EBS amplitude of the all DNA substrate, which was 25 pA in buffer containing 0.3 M KCl and 19 pA in buffer containing 0.15 M KCl.

to dCMP at $n = 0$ in the KF active site), DNA−KF complexes remained fixed at the same position relative to the nanopore for an average of ~150 ms,[9] allowing accurate current measurements. A current trace showing representative events (Figure 3c) and a plot of dwell time *versus* current levels (Figure 3d) reveal that when ternary complexes formed with the 12ab(12,23) substrate are captured the EBS median amplitude is 38 pA. This is 13 pA higher than for complexes formed with the DNA control substrate (25 pA). This effect of the 12ab(12,23) substrate on current level was observed only in the EBS and not in DNA capture events for this substrate absent KF (data not shown) nor in the terminal steps of enzyme-bound events (Figure 3d, gray points). Thus, a 12 abasic block in template DNA causes a significant difference in ionic current relative to a DNA control when captured in the nanopore, consistent with predictions based on structural data.

To further localize the influence of abasic residues on ionic current amplitude, we examined two DNA templates bearing six abasic inserts, 6ab(18,23) and 6ab(12,17), corresponding to the halves of the 12 abasic modification (Figure 2, templates C and D). Most of the 13 pA difference elicited by the 12ab(12,23) substrate could be attributed to the abasic residues present in the 6ab(12,17) template. Capture of ternary complexes formed with this substrate resulted in 35 pA residual current, compared to 28 pA for complexes formed with 6ab(18,23).

Mapping Template Position at Single Nucleotide (~5 Å) Precision. We then determined the effect of inserts composed of three abasic residues on ionic current across the nanopore. We had two specific goals: (1) establish a more precise map of the influence of abasic inserts on nanopore current; and (2) determine if single nucleotide displacement of these inserts could be detected at high bandwidth, thus enabling single molecule experiments on abasic-containing template displacement during synthesis. To generate a fine-grained map in the region predicted to be most sensitive to abasic residues, the three abasic inserts were offset by a single nucleotide, such that two of three abasic residues overlapped in neighboring templates (Figure 2, templates E−Q).

Results of experiments using DNA templates bearing three abasic inserts are shown in Figure 4. In these experiments, the DNA templates were hybridized to 23mer 2′,3′-dideoxy-terminated primers. Representative current traces (Figure 4a) and corresponding dwell time *versus* amplitude plots for individual complexes (Figure 4b) reveal ionic current changes dependent upon the position of the three abasic inserts. For example, placement of the insert at positions +10 to +12 distal from the catalytic site (substrate 3ab(10,12)) results in $I_{EBS} = 36$ pA (Figure 4a,b). This is 11 pA greater than I_{EBS} for the all DNA template control and close to I_{EBS} for the 12 abasic insert (Figure 3), indicating that

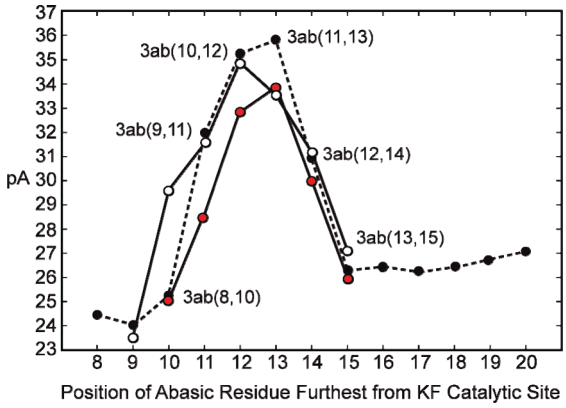

Figure 5. Amplitude map for three abasic residue inserts for KF complexes with substrates bearing 22mer or 24mer duplex regions. Amplitude levels, measured in buffer containing 0.3 M KCl, for DNA−KF−dGTP ternary complexes with substrates bearing the indicated three abasic residue insert configurations, hybridized with 22mer (red circles, solid line), 23mer (black circles, dashed line), or 24mer (open circles, solid line) 2′,3′-dideoxy-terminated primers. The location of the abasic insert in the nanopore lumen is determined by the enzyme bound at the double strand−single strand junction of the substrate, measured as it is held in a fixed position atop the nanopore. Therefore, to achieve the same abasic configuration with different length primers, they must be hybridized to different templates. Thus, for the abasic configuration 3ab(11,13) with a 23mer primer, template J (Figure 2) is used, while the 22mer and 24mer primers require templates I and K (Figure 2), respectively.

most of the change in resistance is due to a short segment of abasic residues close to the limiting aperture of α-HL. Displacing the three abasic insert closer to the catalytic site by a single nucleotide (to positions +9 to +11 (substrate 3ab(9,11)) results in a decrease to I_{EBS} = 32 pA (Figure 4a,b). Displacement of the abasic insert one step further, to positions +8 to +10 (substrate 3ab(8,10)), results in ternary complexes with $I_{EBS} \sim 26$ pA, nearly the same as the all DNA substrate. Thus, movement of a three abasic segment within a DNA template in single nucleotide steps (~5 Å) yields up to a 6 pA current difference that is detectable at 10 kHz bandwidth. A map of ionic current as a function of the three abasic position along the DNA template (Figure 4c, solid line) indicates that other single nucleotide displacements (*e.g.*, movement from 3ab(13,15) to 3ab(12,14) to 3ab(11,13)) cause I_{EBS} changes on the order of 5−6 pA. Ionic current measurements for hundreds of capture events were highly reproducible for each substrate, indicating little deviation in the position of the KF-bound template relative to α-HL. Current blockade level variation from experiment to experiment was within ±1 pA for each substrate.

Current Amplitude Map in 0.15 KCl Buffer. In the preceding experiments, I_{EBS} maps were generated in buffer containing 0.3 M KCl. These maps could be used to monitor KF function on the nanopore because KF catalytic activity is retained under these conditions.[8] However, elevated levels of monovalent salts can diminish KF function[21,22] and are likely to inhibit the activity of other mesophilic DNA and RNA processing enzymes. Thus, to establish broader utility for this technique, we repeated these measurements for KF ternary complexes in buffer containing 0.15 M KCl. In this lower salt buffer, the signal-to-noise ratio was sufficient to accurately differentiate between the EBS and terminal step of capture events. We found that the I_{EBS} map in 0.15 M KCl buffer mirrored the I_{EBS} map in 0.3 M KCl buffer for KF ternary complexes with DNA substrates bearing abasic inserts at the most sensitive region of the nanopore lumen (Figure 4c).

Detection of Primer Extension Using the Sanger Method. The biochemical strategy employed in the Sanger sequencing method relies upon DNA polymerase extension of primers in the presence of dNTPs and each of four ddNTPs added to separate reaction vessels.[20] In each mixture, primer extension truncates at discrete positions defined by the base identity of the ddNTP and the DNA template that is copied. The ddNTP/dNTP ratio determines the likelihood of truncation at a given complementary base. This results in base-specific DNA ladders that can be resolved and visualized by gel separation.[20]

The ionic current map in Figure 4c predicts that the nanopore could detect primer extension products generated using the Sanger method. To test this prediction, it was first necessary to establish I_{EBS} amplitudes for ternary complexes wherein templates bearing three abasic inserts were hybridized to DNA primers that would precisely mimic products of primer extension. In other words, it was important to demonstrate that ionic current reported by abasic insert position was not significantly altered by other variables including duplex product length, sequence identity in the polymerase catalytic site, and DNA sequence identity flanking the abasic insert.

For this test, the abasic-bearing DNA templates examined in Figure 4 were hybridized to 22mer or 24mer 2′,3′-dideoxy-terminated primers. I_{EBS} values for these substrates as ternary complexes with KF and dGTP were then compared to I_{EBS} values for the 23mer ternary complexes reported above. We found that the three maps nearly superimposed (Figure 5), with I_{EBS} peaks of similar magnitude centered around the same abasic configurations. Variables including duplex length and nucleotide identity in the KF catalytic site had reproducible but minor effects on I_{EBS}. Thus, as primer length increases from 22 to 23 to 24 nucleotides, each sequence of three map positions represents a snapshot of ternary complex amplitudes. For example, a complex formed with template K (Figure 2) hybridized to a 22mer primer has the abasic configuration 3ab(13,15) and an amplitude of ~26 pA. This same template with a 23mer primer has an abasic configuration of 3ab(12,14) and amplitude of 31.5 pA. This ternary complex represents the polymerase advanced on the template by one nucleotide relative to the 22mer complex. The complex with the 24mer duplex on template K

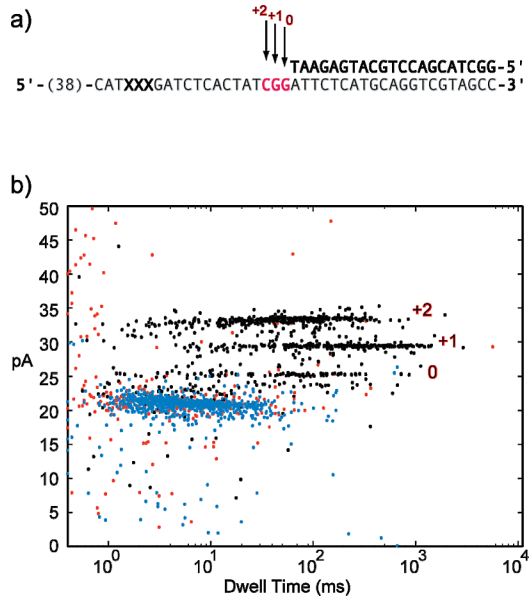

Figure 6. Detection of primer extension using the Sanger method. (a) Template K, modified to contain a G at position $n = 0$ instead of a C, annealed to a 21mer primer with a 3′-OH terminus. The positions 0, +1, and +2 correspond to extension of the 21mer primer to the length of 22, 23, and 24 nucleotides, respectively. (b) Dwell time *vs* amplitude plot showing the ternary complex populations that emerged when the primer template substrate in panel a was added to the *cis* compartment along with 1 μM KF, 400 μM ddCTP, 2.5 μM dCTP, 400 μM ddGTP, 200 μM dATP, and 5 mM $MgCl_2$. To achieve the 0 population, a single ddCTP must be incorporated into the primer strand. For the +1 population, dCTP must be added at the 0 position, followed by ddCTP addition at the +1 position. Finally, the +2 population corresponds to addition of two consecutive dCTP residues followed by ddGTP addition.

(configuration 3ab(11,13)) corresponds to one further step by the enzyme complex and yields an amplitude of almost 34 pA. In summary, position of the three abasic insert dominates the observed current for a given DNA substrate. These amplitudes are therefore what we would expect as KF progresses on a single template, drawing the template up through the nanopore in single nucleotide steps.

Our next goal was detection of KF-dependent extension products bearing 22, 23, or 24mer 2′,3′-dideoxy-terminated primer strands, produced enzymatically in the nanopore chamber using the Sanger method. In this experiment, the starting substrate was a 21mer primer with a 3′-OH terminus annealed to a template similar to template K (Figure 2) but modified to contain a guanosine (G) base at position $n = 0$ (Figure 6a). The next template base (position $n = +1$) is also G, followed by C at position +2 (Figure 6a). When [ddCTP] ≫ [dCTP] and ddGTP and dATP are also present, three nucleotides can be added to this substrate during primer extension. Due to the excess of ddCTP over dCTP, a portion of the extended primers is expected to truncate at 22 or 23 nucleotides in length, despite the ~1000-fold preference of KF for dNTP over ddNTP substrates.[23] The resulting dideoxy-terminated strands can then form stable ternary complexes with KF and the next complementary nucleotides.

When this substrate with the 21mer duplex was added to the nanopore *cis* compartment in the presence of 1 μM KF, 400 μM ddCTP, 2.5 μM dCTP, 400 μM ddGTP, and 200 μM dATP, three major populations of events emerged. These populations at 26, 29, and 33 pA (labeled 0, +1, and +2; Figure 6b) correspond closely to the ternary complex amplitudes measured for template K hybridized to 22, 23, and 24mer primers, respectively (Figure 5). Thus the DNA ladder generated on separate templates in Figures 4 and 5 was reproduced catalytically in the nanopore chamber using the Sanger method.

Comparison of T7 DNA Polymerase and KF. In 0.15 M KCl, I_{EBS} for KF ternary complexes plotted as a function of three abasic insert position mirrored the I_{EBS} plot in 0.3 M KCl buffer (Figure 4c). We used this detection capability in 0.15 M KCl buffer to examine complexes of bacteriophage T7 DNA polymerase with DNA substrates containing abasic inserts (Figures 7 and 8). A representative current trace for a complex captured in the presence of 1 μM DNA (3ab(12,14) with a 23mer 2′,3′-dideoxy primer), 1 μM T7 DNA polymerase, 12 μM thioredoxin, and 200 μM dGTP is shown in Figure 7a. Thioredoxin is an *E. coli* protein that forms a 1:1 complex with the bacteriophage polymerase and increases its processivity.[24] This current trace shares features of current traces for KF ternary complexes with the same three abasic substrate, that is, an initial current blockade at ~23 pA (Figure 7a,i) followed by a brief current reduction to ~17 pA and then a return to 31 pA (Figure 7a,iii). This event structure indicates that, when T7 DNA polymerase complexes are captured by the α-HL nanopore, a series of events ensues that is similar to the series observed for captured KF complexes. That is, an EBS (Figure 7a,i) is followed by voltage-promoted enzyme dissociation allowing the duplex DNA segment to drop into the pore vestibule (Figure 7a,ii), which is followed by DNA translocation through the nanopore.

A plot of dwell time *versus* amplitude for capture events in the presence of DNA, T7 DNA polymerase, and thioredoxin (absent dGTP) shows an EBS cluster with median duration of 1.9 ms (Figure 7b). In the presence of 300 μM each of dATP, dCTP, and dTTP, the median dwell time of events was not significantly changed (3.1 ms; Figure 7c). Subsequent addition of 300 μM dGTP (complementary to dCMP at $n = 0$ in the polymerase active site) yielded a population of EBS events with a median dwell time of 16.7 ms (Figure 7d). This sequence-specific increase of dwell time indicates formation of a quaternary complex with the correct incoming dNTP in the polymerase active site, analogous to the KF ternary complex.[8,9] We note, however, that dwell times for T7 DNA polymerase complexes were notably shorter than for KF complexes at the same dGTP concentration (see Discussion).

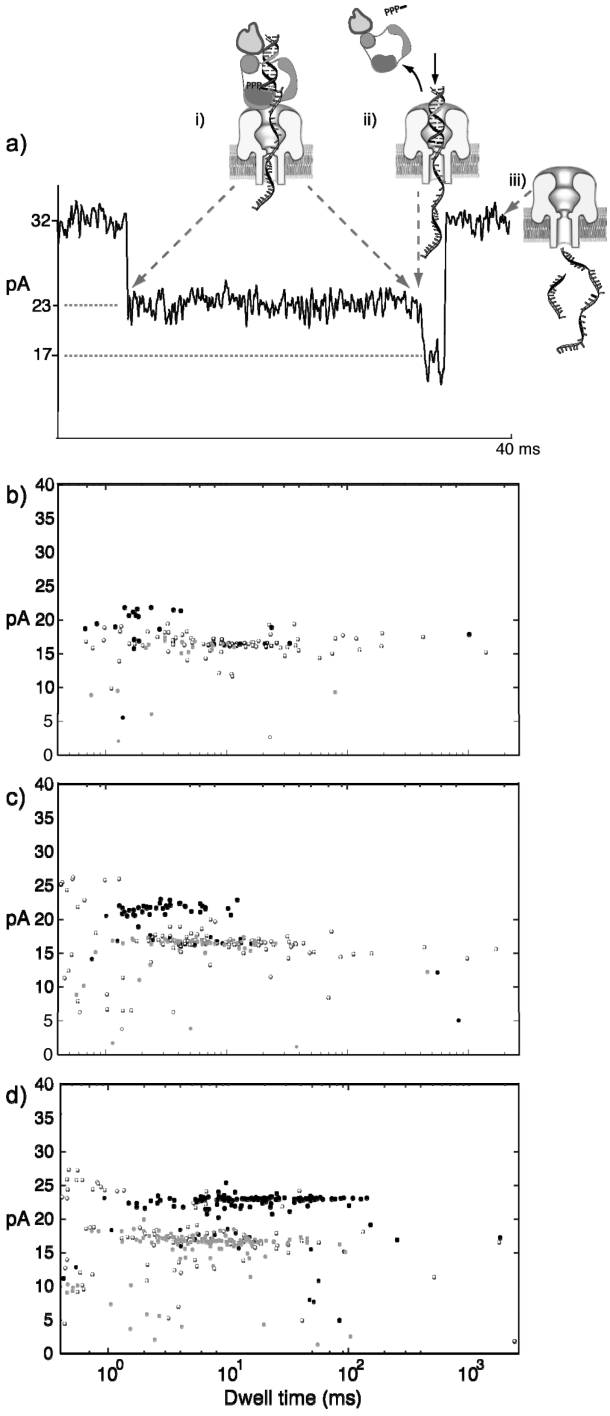

Figure 7. Capturing T7 DNA polymerase complexes in the nanopore. (a) Representative current trace at 180 mV for nanopore capture of a DNA−T7 DNA polymerase−thioredoxin complex, measured in buffer containing 0.15 M KCl. The DNA substrate has the abasic configuration 3ab(12,14), hybridized with a 23mer primer. Cartoons illustrate the molecular events corresponding to each current level. (i) Initial enzyme-bound state (EBS), with the duplex DNA held atop the nanopore in a complex with T7 DNA polymerase and thioredoxin, is followed by (ii) a ~17 pA terminal step when the complex dissociates and the duplex DNA enters the nanopore vestibule. (iii) DNA strands translocate through the nanopore, restoring the open channel current. (b−d) Sequence-specific capture of T7 DNA polymerase quaternary complexes. Dwell time *vs* amplitude plots of capture events in the presence of (b), DNA (3ab(12,14), hybridized with a 23mer primer), T7 DNA polymerase, and thioredoxin, followed by addition of (c) dATP, dCTP, and dTTP (300 μM each), and then (d) 300 μM dGTP.

We next measured current amplitudes for T7 quaternary complexes formed with the six 23mer duplex substrates that defined the peak in the KF ternary complex map. For each substrate, I_{EBS} levels for T7 quaternary complexes were nearly identical to those determined for KF ternary complexes in 0.15 M KCl buffer (Figure 8a). To test this more rigorously, we exploited the difference in median dwell time elicited by the same dGTP concentration for KF and T7 DNA polymerase. This allowed us to examine the two enzymes on the same pore within the same experiment (Figure 8b,c). We used the 3ab(12,14) substrate because its displacement by 5 Å in either direction within the nanopore lumen yields changes of 3−5 pA in 0.15 M KCl buffer, making it ideal for monitoring possible differences between the two enzymes. Median dwell time and amplitude for EBS events measured in the presence of DNA, T7 DNA polymerase, thioredoxin, and 200 μM dGTP were 9.9 ms and 22.2 pA, respectively (Figure 8b). Upon addition of KF, a population of longer dwell time EBS events emerged, bringing the median for the mixed population to 243 ms. The median amplitude for this population was 22.7 pA (Figure 8c), not significantly different from the amplitude measured in the presence of T7 DNA polymerase alone. In summary, this nanopore assay indicates with 5 Å precision that these two structurally conserved polymerases are captured such that the position of the bound template in the pore lumen is the same.

DISCUSSION

We have developed a nanopore method to monitor the position of individual DNA substrates bound to DNA polymerases at single nucleotide (5 Å) precision. As a three abasic insert is displaced in single nucleotide steps toward the active site of the enzyme atop the nanopore, the resulting I_{EBS} map has a single peak (Figures 4c, 5, and 8a). Two displacements of the template toward the vestibule are required to scale this peak, followed by a single displacement that retains the same I_{EBS} level, and then two further displacements that ultimately yield I_{EBS} levels ≃ to an all DNA substrate. This suggests a region of the nanopore lumen that is sensitive to the reduced volume occupied by abasic residues. This current-sensitive region of the nanopore lumen was similar for ternary complexes in which primer length, sequences flanking the abasic insert, and sequences proximal to the polymerase active site were varied (Figure 5). Modest I_{EBS} differences between DNA substrates with the same abasic configuration may be due to these factors and prove informative in future studies.

The spatial precision and reproducibility of the nanopore measurements were readily established

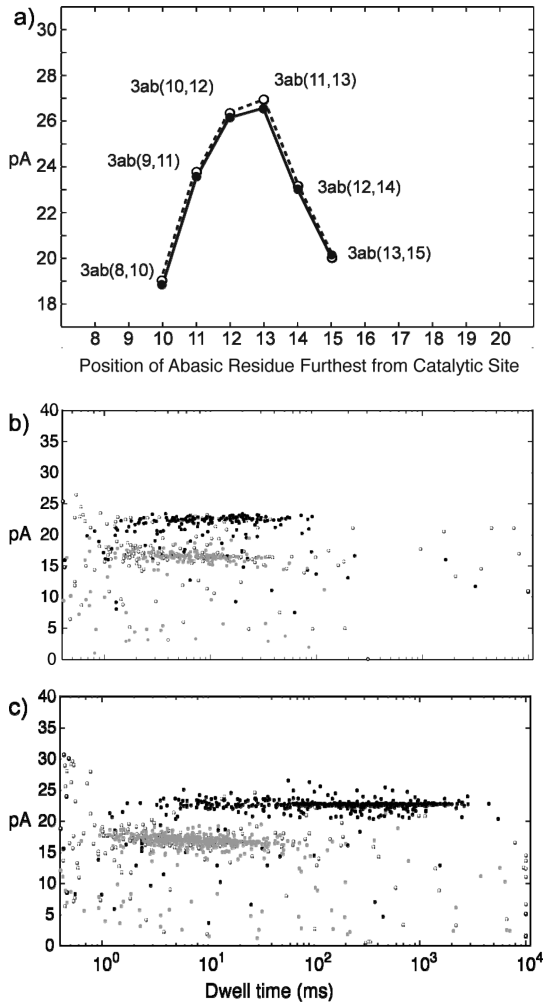

Figure 8. Current amplitudes for templates with three abasic residue inserts bound in T7 DNA polymerase quaternary complexes. (a) Amplitude map measured in buffer containing 0.15 M KCl, for substrates bearing the indicated three abasic residue insert configurations, in quaternary complexes of DNA−T7 DNA polymerase−thioredoxin−dGTP (closed circles, solid line), or ternary complexes of DNA−KF−dGTP (open circles, dashed line). (b,c) Direct comparison of KF and T7 DNA polymerase complexes. Dwell time *vs* amplitude plots are shown for events with (b) DNA (abasic configuration 3ab(12,14), hybridized with a 23mer primer), T7 DNA polymerase, thioredoxin, and dGTP present in the nanopore chamber and (c) after subsequent addition of KF. Control experiments showed that the presence of thioredoxin and DTT, required for the T7 DNA polymerase experiment, did not affect the dwell time or amplitude of KF events (not shown).

because I_{EBS} and dwell time values for hundreds of individual complexes could be determined in real time and compiled within minutes (Figures 4, 7, and 8). These features allowed us to perform enzyme-dependent primer-extension experiments (analogous to the Sanger method) in the *cis* chamber bathing the nanopore. In these experiments, sequential nucleotide addition by KF to a primer/template substrate and the attendant displacement of the three abasic insert relative to the pore lumen resulted in a discrete I_{EBS} ladder (Figure 6b). These I_{EBS} values mirrored those measured for chemically synthesized DNA substrates with abasic inserts at defined distances from the KF catalytic site (Figure 6).

The nanopore experiments were performed using 0.3 M KCl buffer to optimize detection of polymerase−DNA−dNTP complexes or using 0.15 M KCl buffer to optimize polymerase function. The ability to detect capture of these complexes in 0.15 M KCl will enable precision nanopore experiments for a wide range of mesophilic enzymes. Ghadiri and colleagues[7] used buffer containing 0.15 M KCl to detect the addition of nucleotides to a primer/template substrate by a modified version of *Thermus aquaticus* DNA polymerase. In that study, the products of nucleotide addition were detected when the unbound DNA duplex was drawn into the pore vestibule at 30 min intervals;[7] therefore, discrimination between functional states of enzyme complexes or between enzyme-bound and unbound DNA was unnecessary. In contrast, monitoring DNA synthesis by polymerases held atop the nanopore will likely require discrimination between these states in real time at 5 Å resolution as afforded by the abasic-containing templates.

The close similarity of current traces for events with T7 DNA polymerase (Figure 7a) and KF (Figures 1b, 3c, and 4a), together with the finding that the amplitude maps for these enzymes are nearly identical (Figure 8a) reflects the structural conservation of these two A-family polymerases.[4,25,26] It also suggests that these enzymes adopt a similar orientation while they reside on the pore, with the single-stranded template exiting the enzyme at the same distance relative to the catalytic domain.

We have shown that when KF resides in this captured orientation dNTP substrates are iteratively bound and released,[9] satisfying the requirement for a functional active site in order to measure synthesis on the nanopore. The median dwell time elicited by 300 μM dGTP for T7 DNA polymerase complexes (16.7 ms; Figure 7d) was markedly shorter than for KF complexes at the same dGTP concentration (~300 ms).[9] This difference is predicted, at least in part, by the difference in K_d values for dNTP binding to these two enzymes, measured in pre-steady-state kinetic analyses. In those studies, the K_d for dNTP binding to complexes of DNA, T7 DNA polymerase, and thioredoxin was 18 μM,[27] compared to 5 μM for dNTP binding to complexes of DNA and KF.[28] We are using titration experiments and mathematical modeling[9] to probe the detailed kinetic features of substrate binding to T7 DNA polymerase complexes captured on the nanopore. The high processivity of this polymerase in the presence of thioredoxin makes it a good candidate for monitoring single molecule DNA synthesis on the nanopore.

In conclusion, DNA polymerase complexes with their DNA substrates were captured by the applied electric field across an α-HL nanopore. Upon capture, the residual ionic current across the nanopore was influenced by abasic inserts within the DNA template that were positioned

in the pore lumen. Single nucleotide displacements of these abasic inserts within this sensitive region resulted in current differences that were measurable at 5 Å precision in real time. These current differences were used to detect polymerase-dependent extension of DNA primer strands.

METHODS

Materials. Klenow fragment (exo-) was from New England Biolabs (100 000 U mL^{-1}; specific activity 20 000 U mg^{-1}). T7 DNA polymerase (Sequenase Version 2.0, 45 U μL^{-1}) was obtained from USB. *E. coli* thioredoxin was from Promega. Deoxynucleoside triphosphates (dNTPs) were from GE Healthcare Life Sciences. DNA oligonucleotides were synthesized by Stanford University Protein and Nucleic Acid Facility using D-spacer phosphoramidites (Glen Research) and were purified by denaturing PAGE. Primer/template hybrids were formed as described.[8]

Nanopore Methods. The nanopore device and insertion of a single α-HL channel in a lipid blayer have been described.[17,18] Ionic current flux through the α-HL nanopore was measured using an Axopatch 200B integrating patch-clamp amplifier (Molecular Devices) in voltage-clamp mode at 23 $\pm$ 0.2 °C. Data were acquired with a Digidata 1440A analog-to-digital converter (Molecular Devices) at 20 μs intervals in the whole cell configuration and filtered at 10 kHz using a low-pass Bessel filter. Current blockades were measured at 180 mV (*trans*-side positive).

Biochemical Methods. Experiments were conducted at 23 °C. KF experiments with substrates bearing 23mer primers were conducted using 1 μM of the indicated DNA hybrids, 1 μM KF, and 200 μM dGTP (unless otherwise noted) in 10 mM HEPES/KOH, pH 8.00 $\pm$ 0.05, 5 mM $MgCl_2$, and either 0.3 or 0.15 M KCl as indicated in the text and figure legends. T7 DNA polymerase experiments were conducted using 1 μM of the indicated DNA hybrids, 1 μM Sequenase Version 2.0 (containing T7 DNA polymerase and thioredoxin at 1:1 stoichiometry), and 11 μM additional thioredoxin, in 15 mM HEPES/KOH, pH 7.70 $\pm$ 0.05, 5 mM $MgCl_2$, 7 mM DTT, 0.15 M KCl. Map amplitude values were determined using templates generated from 2−3 independent solid-phase synthesis reactions.

Substrates with 22 or 24mer primers were generated in bulk phase in the nanopore chamber by KF-catalyzed addition of the appropriate ddNTP to substrates bearing 3′-OH terminated 21 or 23mer primers, respectively. The reactions used 1 μM 21 or 23mer duplex, 1 μM KF, and 30 μM ddGTP. Ternary complexes were formed by subsequent addition of 200 μM dCTP to the 22mer duplex product or 200 μM dATP to the 24mer duplex product. In each case, emergence of the longer dwell time ternary population was dependent upon the presence of the complementary dNTP, verifying the catalytic addition of the preceding ddNTP.

Data Processing. Current blockade events were identified using MATLAB (2007a, The MathWorks, Natick, MA) and software developed in our laboratory. A capture event was identified when the current level dropped from the open channel current by at least 3 pA for at least 0.2 ms. To quantify the EBS and terminal steps of individual events, a baseline amplitude was calculated as the mean of the first 0.2 ms of the event amplitude. A threshold value for a downward deviation from the baseline amplitude was determined for the terminal step of events by visual inspection of the current traces (as it varied with different abasic substrates depending upon the amplitude of the EBS). Events that ended with a segment below the set threshold were identified as having a terminal step, and the dwell time and mean amplitude for the EBS and terminal step were measured. In the dwell time *versus* amplitude plots generated from this analysis (Figures 3d, 4b, 6b, 7b−d, and 8b,c), black dots represent the EBS of events. In panels 4b and 6b, dots for the terminal steps are blue and events that lack terminal steps are red; in 3d, 7b−d, and 8b,c, terminal step dots are gray and dots for events lacking terminal steps are white with black outline. For each of the current values plotted in this study, the data varied no more than $\pm$1 pA.

Acknowledgment. We are grateful to Nicholas Hurt for early experiments with T7 DNA polymerase, and to Peter Walker for expert oligonucleotide synthesis. This work was supported by a grant from Oxford Nanopore Technologies to M.A. Support for D.G. was provided by a fellowship from NHGRI, Award #5P41HG002371-09.

REFERENCES AND NOTES

1. Dahlberg, M. E.; Benkovic, S. J. Kinetic Mechanism of DNA Polymerase I (Klenow Fragment): Identification of a Second Conformational Change and Evaluation of the Internal Equilibrium Constant. *Biochemistry* **1991**, *30*, 4835–4843.
2. Brautigam, C. A.; Steitz, T. A. Structural and Functional Insights Provided by Crystal Structures of DNA Polymerases and Their Substrate Complexes. *Curr. Opin. Struct. Biol.* **1998**, *8*, 54–63.
3. Li, Y.; Korolev, S.; Waksman, G. Crystal Structures of Open and Closed Forms of Binary and Ternary Complexes of the Large Fragment of Thermus Aquaticus DNA Polymerase I: Structural Basis for Nucleotide Incorporation. *EMBO J.* **1998**, *17*, 7514–7525.
4. Doublié, S.; Tabor, S.; Long, A. M.; Richardson, C. C.; Ellenberger, T. Crystal Structure of a Bacteriophage T7 DNA Replication Complex at 2.2 Å Resolution. *Nature* **1998**, *391*, 251–258.
5. Johnson, S. J.; Taylor, J. S.; Beese, L. S. Processive DNA Synthesis Observed in a Polymerase Crystal Suggests a Mechanism for the Prevention of Frameshift Mutations. *Proc. Natl. Acad. Sci. U.S.A.* **2003**, *100*, 3895–3900.
6. Joyce, C. M.; Potapova, O.; Delucia, A. M.; Huang, X.; Basu, V. P.; Grindley, N. D. Fingers-Closing and Other Rapid Conformational Changes in DNA Polymerase I (Klenow Fragment) and Their Role in Nucleotide Selectivity. *Biochemistry* **2008**, *47*, 6103–6116.
7. Cockroft, S. L.; Chu, J.; Amorin, M.; Ghadiri, M. R. A Single-Molecule Nanopore Device Detects DNA Polymerase Activity with Single-Nucleotide Resolution. *J. Am. Chem. Soc.* **2008**, *130*, 818–820.
8. Benner, S.; Chen, R. J. A.; Wilson, N. A.; Abu-Shumays, R.; Hurt, N.; Lieberman, K. R.; Deamer, D. W.; Dunbar, W. B.; Akeson, M. Sequence-Specific Detection of Individual DNA Polymerase Complexes in Real Time Using a Nanopore. *Nat. Nanotechnol.* **2007**, *2*, 718–724.
9. Hurt, N.; Wang, H.; Akeson, M.; Lieberman, K. R. Specific Nucleotide Binding and Rebinding to Individual DNA Polymerase Complexes Captured on a Nanopore. *J. Am. Chem. Soc.* **2009**, *131*, 3772–3778.
10. Li, J.; Stein, D.; McMullan, C.; Branton, D.; Aziz, M. J.; Golovchenko, J. A. Ion-Beam Sculpting at Nanometre Length Scales. *Nature* **2001**, *412*, 166–169.
11. Meller, A.; Branton, D. Single Molecule Measurements of DNA Transport through a Nanopore. *Electrophoresis* **2002**, *23*, 2583–2591.
12. Kasianowicz, J. J.; Brandin, E.; Branton, D.; Deamer, D. W. Characterization of Individual Polynucleotide Molecules Using a Membrane Channel. *Proc. Natl. Acad. Sci. U.S.A.* **1996**, *93*, 13770–13773.
13. Bayley, H.; Cremer, P. S. Stochastic Sensors Inspired by Biology. *Nature* **2001**, *413*, 226–230.
14. Akeson, M.; Branton, D.; Kasianowicz, J. J.; Brandin, E.; Deamer, D. W. Microsecond Time-Scale Discrimination Among Polycytidylic Acid, Polyadenylic Acid, and Polyuridylic Acid as Homopolymers or as Segments within Single RNA Molecules. *Biophys. J.* **1999**, *77*, 3227–3233.

15. Butler, T. Z.; Pavlenok, M.; Derrington, I. M.; Niederweis, M.; Gundlach, J. H. Single-Molecule DNA Detection with an Engineered Mspa Protein Nanopore. *Proc. Natl. Acad. Sci. U.S.A.* **2008**, *105*, 20647–20652.
16. Song, L.; Hobaugh, M. R.; Shustak, C.; Cheley, S.; Bayley, H.; Gouaux, J. E. Structure of Staphylococcal Alpha-Hemolysin, a Heptameric Transmembrane Pore. *Science* **1996**, *274*, 1859–1866.
17. Vercoutere, W. A.; Winters-Hilt, S.; DeGuzman, V. S.; Deamer, D.; Ridino, S. E.; Rodgers, J. T.; Olsen, H. E.; Marziali, A.; Akeson, M. Discrimination among Individual Watson−Crick Base Pairs at the Termini of Single DNA Hairpin Molecules. *Nucleic Acids Res.* **2003**, *31*, 1311–1318.
18. Vercoutere, W.; Winters-Hilt, S.; Olsen, H.; Deamer, D.; Haussler, D.; Akeson, M. Rapid Discrimination among Individual DNA Hairpin Molecules at Single-Nucleotide Resolution Using an Ion Channel. *Nat. Biotechnol.* **2001**, *19*, 248–252.
19. Meller, A.; Nivon, L.; Brandin, E.; Golovchenko, J.; Branton, D. Rapid Nanopore Discrimination between Single Polynucleotide Molecules. *Proc. Natl. Acad. Sci. U.S.A.* **2000**, *97*, 1079–1084.
20. Sanger, F.; Nicklen, S.; Coulson, A. R. DNA Sequencing with Chain-Terminating Inhibitors. *Proc. Natl. Acad. Sci. U.S.A.* **1977**, *74*, 5463–5467.
21. Turner, R. M.; Grindley, N. D.; Joyce, C. M. Interaction of DNA Polymerase I (Klenow Fragment) with the Single-Stranded Template Beyond the Site of Synthesis. *Biochemistry* **2003**, *42*, 2373–2385.
22. Gangurde, R.; Modak, M. J. Participation of Active-Site Carboxylates of *Escherichia coli* DNA Polymerase I (Klenow Fragment) in the Formation of a Prepolymerase Ternary Complex. *Biochemistry* **2002**, *41*, 14552–14559.
23. Astatke, M.; Grindley, N. D.; Joyce, C. M. How *E. coli* DNA Polymerase I (Klenow Fragment) Distinguishes Between Deoxy- and Dideoxynucleotides. *J. Mol. Biol.* **1998**, *278*, 147–165.
24. Tabor, S.; Huber, H. E.; Richardson, C. C. *Escherichia coli* Thioredoxin Confers Processivity on the DNA Polymerase Activity of the Gene 5 Protein of Bacteriophage T7. *J. Biol. Chem.* **1987**, *262*, 16212–16223.
25. Joyce, C. M.; Steitz, T. A. Function and Structure Relationships in DNA Polymerases. *Annu. Rev. Biochem.* **1994**, *63*, 777–822.
26. Rothwell, P. J.; Waksman, G. Structure and Mechanism of DNA Polymerases. *Adv. Protein Chem.* **2005**, *71*, 401–440.
27. Patel, S. S.; Wong, I.; Johnson, K. A. Pre-Steady-State Kinetic Analysis of Processive DNA Replication Including Complete Characterization of an Exonuclease-Deficient Mutant. *Biochemistry* **1991**, *30*, 511–525.
28. Kuchta, R. D.; Mizrahi, V.; Benkovic, P. A.; Johnson, K. A.; Benkovic, S. J. Kinetic Mechanism of DNA Polymerase I (Klenow). *Biochemistry* **1987**, *26*, 8410–8417.